



CHALMERS
UNIVERSITY OF TECHNOLOGY

Immobilization of bacterial feruloyl esterase on mesoporous silica particles and enhancement of synthetic activity by hydrophobic-modified surface

Downloaded from: <https://research.chalmers.se>, 2026-04-04 14:54 UTC

Citation for the original published paper (version of record):

Chong, S., Cardoso, V., Brás, J. et al (2019). Immobilization of bacterial feruloyl esterase on mesoporous silica particles and enhancement of synthetic activity by hydrophobic-modified surface. *Bioresource Technology*, 293. <http://dx.doi.org/10.1016/j.biortech.2019.122009>

N.B. When citing this work, cite the original published paper.



Immobilization of bacterial feruloyl esterase on mesoporous silica particles and enhancement of synthetic activity by hydrophobic-modified surface



Sun Li Chong^{a,b}, Vânia Cardoso^{c,d}, Joana L.A. Brás^c, Milene Zezzi do Valle Gomes^e, Carlos M.G.A. Fontes^{c,d}, Lisbeth Olsson^{b,*}

^a State Key Laboratory of Subtropical Silviculture, Zhejiang A&F University, Lin'an, 311300 Hangzhou, China

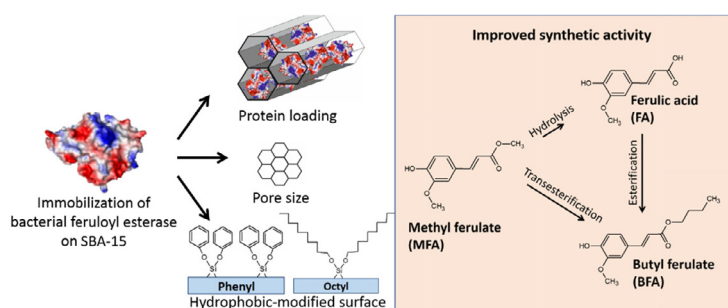
^b Chalmers University of Technology, Department of Biology and Biological Engineering, Division of Industrial Biotechnology, Kemivägen 10, SE-412 96 Göteborg, Sweden

^c NZYTech Genes & Enzymes, Campus do Lumiar, 1649-038 Lisbon, Portugal

^d CHISA – Faculty of Veterinary Medicine, University of Lisbon, 1300-477 Lisboa, Portugal

^e Chalmers University of Technology, Department of Chemistry and Chemical Engineering, Applied Chemistry, SE 412 96 Gothenburg, Sweden

GRAPHICAL ABSTRACT



ARTICLE INFO

Keywords:

SBA-15
Protein loading
Pore size
Butyl ferulate
Transesterification

ABSTRACT

Here, we demonstrated the immobilization of bacterial feruloyl esterase (FAE) from *Butyrivibrio* sp. XPD2006, *Lactobacillus crispatus*, *Butyrivibrio* sp. AE2015, *Ruminococcus albus*, *Cellulosilyticum ruminicola* and *Clostridium cellulovorans* on SBA-15 and their ability to synthesize butyl ferulate (BFA). The BFae2 from *Butyrivibrio* sp. XPD2006 showed the best catalytic efficiency. High BFA yield was produced when the immobilization of BFae2 took place with a high protein loading and narrow pore sized SBA-15, suggesting alteration of enzyme behavior due to the crowding environment in SBA-15. Grafting of SBA-15 with octyl moieties led to shrinking pore size and resulted in 2.5-fold increment of BFA activity compared to the free enzyme and 70%mol BFA was achieved. The BFae2 encapsulated in hydrophobic-modified SBA-15 endured up to seven reaction cycles while the BFA activity remained above 60%. This is the first report showing the superior performance of hydrophobic-modified surface to entrap FAE to produce fatty phenolic esters.

1. Introduction

Ferulic acid and other hydroxycinnamic acids are phytochemicals that exhibit antioxidant activity (Srinivasan et al., 2007). Biocatalytic

modification of hydroxycinnamate with hydrophilic or hydrophobic moieties is anticipated to improve their bioavailability leading to their potential utilization by the pharmaceutical, food and cosmetic industries. Feruloyl esterase (FAE) catalyzes the hydrolysis of an ester

* Corresponding author.

E-mail address: lisbeth.olsson@chalmers.se (L. Olsson).

<https://doi.org/10.1016/j.biortech.2019.122009>

Received 24 June 2019; Received in revised form 11 August 2019; Accepted 12 August 2019

Available online 14 August 2019

0960-8524/ © 2019 The Authors. Published by Elsevier Ltd. This is an open access article under the CC BY-NC-ND license

(<http://creativecommons.org/licenses/by-nc-nd/4.0/>).

linkage between the hydroxycinnamates and plant cell wall polysaccharides (MacKenzie et al., 1987; MacKenzie and Bilous, 1988), primarily xylans and pectins (Oosterveld et al., 2000). They also synthesize hydroxycinnamate fatty esters via transesterification/esterification when the enzymatic reaction takes place in organic solvents (Topakas et al., 2007). Despite being considered to be an unsuitable reaction medium for biocatalysts, organic solvents offer several advantages over aqueous media for synthetic reactions, which include (i) better solubility for organic donor/acceptors, (ii) the development of new reactions, and (iii) the promotion of thermodynamics to reactions unfavorable in aqueous solution (Klibanov, 2001).

Enzymes have evolved to perform reactions in aqueous solutions and thus require water to maintain their native conformation (Zaks and Klibanov, 1985). The use of organic solvents with a limited aqueous buffer for synthetic reactions is likely to distort protein conformations, causing enzyme instability and consequent poor performance. Confining the enzyme to a porous environment will protect the protein molecule from the surrounding bulk solvent (Hartmann and Kostrov, 2013). Mesoporous silica particles (MPS) offer the advantage of a highly specific surface area and controllable pore size, and thus they are highly suitable for enzyme immobilization (Zhou and Hartmann, 2012). Various methods, e.g., physical absorption, covalent bonding, and cross-linking have been employed to immobilize enzymes (Secundo, 2013), and physical absorption is the most classical method that is less prone to protein structural distortion than covalent bonding.

Several factors will influence the catalytic efficiency of the immobilized enzyme. Enzyme immobilization is greatly influenced by pH buffer conditions since protein absorption is predominantly governed by electrostatic interactions (Secundo, 2013). Thus, the amount of protein loaded on MPS reflects the surface net charge of the protein molecules. Since the pH for maximal protein loading may not necessarily lead to optimal catalytic activity (Thörn et al., 2013), it is important to experimentally determine the pH that satisfies the requirement for both optimal protein loading and catalytic activity. The physicochemical properties of MPS can also be manipulated to fine-tune the catalytic activity of the immobilized enzyme. Notably, the pore size not only affects the transport of protein molecules into and out of porous particles (Gustafsson et al., 2011) but also greatly affects the behavior of protein folding that is influenced by the accessible volume in the pore environment (Zhou and Dill, 2001). In addition to geometrical effects, the surface chemistry of MPS has been exploited to enhance enzymatic activity. The most classic example is the use of a hydrophobic surface for the activation of lipase esterification activity. Since the catalytic site of the lipase molecule is covered by a large patch of hydrophobic peptides, functionalizing the silica support with a hydrophobic group such as an octyl would uncover the hydrophobic lid to facilitate the accessibility of the substrate (Fernandez-Lafuente et al., 1998).

Fungal feruloyl esterases (EC 3.1.1.73), also known as ferulic acid esterases (FAEs), confined in SBA-15, a type of MPS constituted by hexagonal ordered silica, demonstrated higher specificity towards synthetic reactions compared to their counterparts in the free form (Hüttner et al., 2017; Thörn et al., 2011). In addition, the immobilized FAEs were highly stable and able to endure multiple reaction cycles. Therefore, immobilizing FAEs in SBA-15 can be a strategy to stabilize the enzyme and to facilitate enzyme recovery when one wants to use the enzyme for several production cycles. The immobilization, however, has not been tested on FAEs originating from bacterial sources.

In the present study, we analyzed the effect of immobilization on the synthetic activity of six recombinant bacterial FAE from *Butyrivibrio* sp. *XPD2006* (BFae2), *Lactobacillus crispatus* (LcFae8), *Butyrivibrio* sp. *AE2015* (BFae9), *Ruminococcus albus* (RaFae), *Cellulosilyticum ruminicola* (CrFae) and *Clostridium cellulovorans* (CcFae); and their ability to perform synthetic reaction in a water-limited reaction system to produce butyl ferulate. The immobilization condition was optimized through varying buffer pH, protein loading and physicochemical

properties of SBA-15, i.e. pore sizes and morphologies; and hydrophobic-modified surfaces. The synthetic activity of the immobilized enzyme was compared to its free form, and the enzyme reusability was evaluated. This is the first report thus far that evaluates the influence of enzyme immobilization on the synthetic activity of bacterial FAEs. We found that the use of SBA-15 with the hydrophobic-modified surface is highly suited for encapsulating bacterial FAEs.

2. Materials and methods

2.1. Materials

Pluronic™ P123 (EO₂₀PO₇₀EO₂₀, Mw = 5800), 1,3,5-trimethylbenzene (TMB, 98%), tetraethylorthosilicate (TEOS, ≥98%), hydrochloric acid (HCl) (37 wt%), ammonium fluoride (NH₄F, ≥99.9%), octyltriethoxysilane (OCTS, ≥97.5%), phenyltriethoxysilane (PHTS, ≥98%) toluene anhydrous (99.8%), anhydrous 1-butanol, citric acid, sodium phosphate dibasic and tris(hydroxymethyl)aminomethane were obtained from Sigma-Aldrich (Saint-Louis, USA). Methyl ferulate (MFA), butyl ferulate (BFA) and ferulic acid (FA) were obtained from Apin Chemical Ltd. (Oxon, United Kingdom).

2.2. Synthesis of mesoporous silica particles

SBA-15 (SBA = Santa Barbara Amorphous) with pore sizes of 7.8, 8.7 and 10 nm were synthesized as described by Gustafsson et al. (2011) using Pluronic™ P123 as the template and TEOS as the silica source. MCF (Mesostructured Cellular Foam) was synthesized as described by Schmidt-Winkel et al. (2000) using TMB as a swelling agent to obtain a pore size of 26.5 nm and a window size of 10.9 nm. The method described in Gomes and Palmqvist (2017) was used to functionalize 10 nm pore size SBA-15 with octyl (SBA-OC) and phenyl (SBA-PH) moieties using OCTS and PHTS as modification agents, respectively. The physical properties of the MPS (Table 1) were characterized using nitrogen gas adsorption analysis. Prior to the adsorption measurements, the non-functionalized MPS were outgassed for at least 8 h at 180 °C, while the functionalized SBA-15 was outgassed overnight at 120 °C. The pore size for SBA-15 was calculated using the BJH (Barrett-Joyner-Halenda) method (Barrett et al., 1951), while the pore and window size distributions for the MCF were calculated using the simplified BdB (Broekhoff-deBoer)-FHH (Frenkel-Halsey-Hill) method (Brunauer et al., 1938; Lukens et al. 1999). The pore volume was calculated using a single point adsorption value at the relative pressure of 0.990.

2.3. Gene synthesis, protein expression and purification

Six bacterial FAEs from *Butyrivibrio* sp. *XPD2006* (BFae2; accession number WP_022766750.1), *Lactobacillus crispatus* (LcFae8; accession number WP_005721797.1), *Butyrivibrio* sp. *AE2015* (BFae9; accession number WP_022776254.1), *Ruminococcus albus* (RaFae; accession number EGC03123.1), *Cellulosilyticum ruminicola*, (CrFae; accession number ACZ98648) and *Clostridium cellulovorans* (CcFae; accession number ADL52399) were produced recombinantly in *Escherichia coli* (*E. coli*). The codons of the six bacterial genes were optimized for

Table 1

Physical properties of SBA-15 and MCF determined by nitrogen adsorption analysis.

MPS	Pore size (nm)	BET surface area (m ² g ⁻¹)	Pore volume (cm ³ g ⁻¹)
SBA-15	7.8	703	1.09
SBA-15	8.7	546	1.25
SBA-15	10	434	1.09
MCF	26.5/10.9	523	1.94
SBA-OC	8.7	444	1.12
SBA-PH	8.2	461	0.94

expression in *E. coli* using ATGenium (NZYTech Ltd., Lisbon, Portugal) codon optimization software. Synthetic genes included the HTP recombinant sequences for direct cloning into the bacterial expression vector pHTP1. The six recombinant plasmids encoding the bacterial FAEs were fused to an N-terminal His₆-tag to facilitate purification using Immobilized Affinity Chromatography (IMAC). The six plasmids were sequenced to ensure that no mutations accumulated during the gene cloning and were used to transform *E. coli* BL21 (DE3) cells. Recombinant *E. coli* cells were grown in NZY Auto-Induction LB medium (NZYTech Ltd., Lisbon, Portugal) supplemented with kanamycin (50 µg/mL) at 37 °C to an early-exponential phase ($A_{600nm} = 1.5\text{--}2.0$), and recombinant protein production occurred following further incubation at 25 °C for 16 h. Recombinant *E. coli* cells were harvested using centrifugation at $75,000 \times g$ at 4 °C for 15 min and lysed in NZY Bacterial Cell Lysis Buffer (NZYTech Ltd., Lisbon, Portugal). The His₆-tagged recombinant FAEs were purified from cell-free extracts using IMAC as described previously (Sequeira et al., 2016). Recombinant proteins were eluted in 50 mM Na HEPES, pH 7.5, 500 mM NaCl, and 300 mM imidazole. The homogeneity of the purified proteins and the molecular mass of the recombinant FAEs were determined using SDS-PAGE. The protein concentration of the FAEs stock solutions varied between 0.5 and 3 mg/mL as determined spectrophotometrically.

2.4. Immobilization of bacterial FAEs in MPS

Prior to enzyme immobilization, the MPS were washed five times in immobilization buffer, i.e., 50 mM citrate-phosphate buffer (pH 5, 6 and 7) or 100 mM Tris (pH 8 and 9). The FAE stocks were buffer-exchanged five times using an Amicon 10 kDa cut-off filter and diluted to the desired protein concentration using immobilization buffer. The protein concentration was determined either using the Bradford assay (Bradford, 1976) or Nanodrop spectrophotometer. For enzyme immobilization, an aliquot of 0.35 mL enzyme sample was added into an Eppendorf tube containing 1.25 mg MPS and mixed overnight on a rotating wheel at 4 °C. The immobilized enzyme-MPS was washed using the solvent-rinsed enzyme preparations (PREPs) method described by Hüttner et al. (2017). Briefly, washing steps were carried out by rinsing three times in immobilization buffer and three times in 1-butanol/buffer (92.5:7.5, v/v). After each washing step, the enzyme-MPS was centrifuged at $12,000 \times g$, and the supernatant was harvested and stored at 4 °C or -20 °C until later use to determine protein leakage. The collected supernatant was dried to completion using either freeze-drying or evaporation using a MiVac sample concentrator (SP scientific, Warminster, USA), reconstituted in 0.1 mL water and subjected to protein measurement using a Nanodrop spectrophotometer. The immobilization efficiency was determined by subtracting the initial protein concentration from the protein remaining after immobilization and leakage in wash buffers. These values were compared to the protein concentration prior to immobilization and expressed as percentages. The protein loading was determined by dividing the amount of immobilized protein present in the support material after multiple washing steps over the MPS used and expressed as $\text{mg}_{\text{protein}} \text{g}_{\text{MPS}}^{-1}$.

2.5. Synthesis of butyl ferulate using free and immobilized bacterial FAEs

The synthesis of butyl ferulate was conducted by mixing the enzyme-MPS in 0.5 mL 1-butanol/buffer (92.5:7.5, v/v) supplemented with 30 mM MFA. The performance of the free enzyme was examined concurrently using an equal amount of protein as that used for the immobilization. Free FAEs were buffer-exchanged five times using an Amicon 10 kDa cut-off filter, adjusted to the desired protein concentration using a buffer, and an aliquot of 0.0375 mL enzyme sample was added to 0.463 mL 1-butanol supplemented with 30 mM MFA. The mixture was incubated at 30 °C in a thermomixer shaken at 14000 rpm. To examine the product profile throughout the course of the enzymatic

reaction, an aliquot of 0.03 mL supernatant was withdrawn at different time points, mixed with 0.07 mL glacial acetic acid to terminate the enzymatic reaction, diluted in 0.4 mL methanol and stored at -20 °C prior to HPLC analysis.

2.6. Determination and calculation of the BFA, FA and MFA reactant products

The amounts of MFA, FA and BFA were measured using C18 HPLC as described by Thörn et al. (2011). Briefly, a 5 µL sample was injected into the HPLC (Dionex-Ultimate 3000) and separated on a C18 column (Kinetex® 2.6 µm, 100 Å, 100 × 4.6 mm) at a flow rate of 1 mL/min utilizing methanol:3.33% acetic acid (70:30; v/v) as the mobile phase. The column oven was maintained at 40 °C. The eluted compound was detected using a UV detector at 300 nm. The amounts of BFA, FA and MFA were determined against calibration curves established by BFA (0.1–20 mM), FA (0.1–20 mM) and MFA standards (0.5–30 mM). The specific BFA/FA activity of the immobilized enzyme was defined by µM BFA/FA produced in a minute and normalized by the amount of protein (mg) and MPS (mg) used in a reaction. The % mol of BFA, FA or MFA was calculated by comparing the molar amount of BFA, FA or MFA to the total molar amount of MFA + FA + BFA and expressed as percentage.

2.7. Reusability

The reusability of the immobilized enzyme was examined by repeating > 4 cycles of BFA synthesis at pH 7. Each reaction cycle lasted 24 h. Before starting every new cycle, the MPS-enzyme was centrifuged, and the supernatant was discarded. The MPS-enzyme was then washed 3 times in 1-butanol/citrate-phosphate buffer, pH 7 (92.5%/7.5%; v/v) to remove any remaining substrates and reactant products. Subsequently, a fresh aliquot of 0.5 mL 30 mM MFA in 1-butanol/citrate-phosphate buffer, pH 7 (92.5%/7.5%; v/v) was added, and the reaction mixture was incubated further at 30 °C in a thermomixer shaken at 14000 rpm. The formation of the reactant products was determined using the HPLC method described above. The enzyme reusability was tested by comparing the specific BFA activity and the BFA/FA molar ratio relative to that obtained from the first cycle of enzymatic reaction.

2.8. Measurement of protein secondary structure using circular dichroism (CD) spectroscopy

The secondary structure of free and immobilized FAEs was determined using a Chirascan CD spectrometer (Applied Photophysics, Leatherhead, United Kingdom) with a 0.05 mm path length cuvette. The protein samples were diluted to the desired concentration in 10 mM potassium phosphate, pH 7, and scanned from 260 to 190 nm five times. The spectra acquired were then averaged, subtracted from the blank buffer with or without MPS, and smoothed by 4–10 window sizes using the manufacturer's software, Pro-Data Viewer (Applied Photophysics, Leatherhead, United Kingdom).

3. Results and discussion

3.1. The effect of pH on the immobilization of the bacterial FAEs

The pH significantly affects the levels of protein loading in silica support and the respective catalytic activity of the immobilized enzyme (Essa et al., 2007; Gustafsson et al., 2011). It has previously been proposed that the highest immobilization efficiency can be achieved at a pH slightly lower than the isoelectric point (pI) of a protein (Essa et al., 2007; Vinu et al., 2003). Since no similar cases have been reported so far for the immobilization of bacterial FAE, it is important to experimentally determine the optimal pH for the immobilization of the

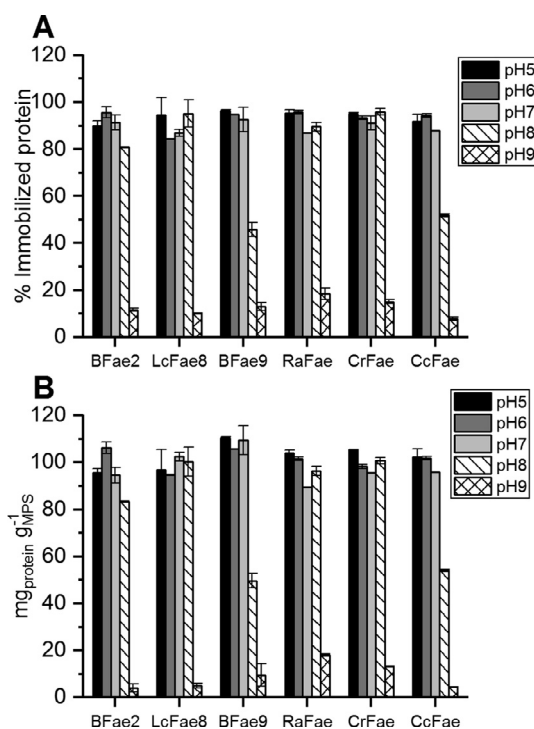


Fig. 1. Immobilization efficiency of the bacterial FAEs on SBA-15 with a pore size of 10 nm. The (A) % Immobilized and (B) protein loading were examined at a pH range from 5 to 9. Error bar represents standard deviation of duplicates.

FAE candidates.

The immobilization efficiency was examined at a pH range from 5 to 9 with the use of 10 nm pore size SBA-15. We found that 80–90% of the proteins were efficiently immobilized across a pH range from 5 to 7 (Fig. 1A), and the attained protein loading ranged from 90 to 110 $\text{mg}_{\text{protein}}/\text{g}_{\text{MPS}}$ (Fig. 1B). In addition, at pH 8, a protein loading of more than 80 $\text{mg}_{\text{protein}}/\text{g}_{\text{MPS}}$ was observed in BFae2, LcFae8, RaFae and CrFae, while the immobilization efficiency for BFae9 and CcFae dropped drastically since only 50% of the proteins were immobilized. At pH 9, the immobilization efficiency decreased to 20% for all the FAEs. The amount of protein leaked in the wash buffer generally ranged 0–4.5% in the pH range 5–8. The leakage was substantial when pH was raised to 9, a range of 12–41% of the protein loaded on MPS leaked from the support material after all six washing steps. A closer inspection of the immobilization profile over a time course of 20 h revealed that the immobilization of most of the protein took place within the initial 30 min of mixing across the pH range from 5 to 9. Enzyme immobilization was close to completion after 1–2 h of mixing since no major improvement was observed when the mixing was prolonged to 20 h. These data were consistent with those reported by Thörn et al. (2011) and Hüttner et al. (2017) that investigated the immobilization of fungal FAEs.

The absorption of proteins to SBA-15 is predominantly governed by electrostatic and to some extent, by van der Waals and hydrophobic interactions (Moerz and Huber, 2014). The interactions are strongly influenced by the pH of the immobilization buffer. SBA-15 has a pI of 3.8 (Essa et al., 2007), and thus the silanol groups on the surface are negatively charged across a pH range from 5 to 9. BFae2, BFae9 and CcFae have a pI ranging from 5.1 to 5.5, while LcFae8, RaFae and CcFae have a slightly higher $pI \approx 6$ (Table 2). All the FAEs exhibited a high immobilization efficiency from pH 5 to 7, which was close to their respective pI . Since the bacterial FAEs are not glycosylated, the protein absorption behavior will be greatly influenced by the net charge present on the naked protein surface rather than by the charge state rendered by the hydrophilic sugar moieties. Therefore, at the pH slightly higher

Table 2

Molecular properties of bacterial FAEs.

Enzyme	pI^a	M_w^b (kDa)	Dimension ^c (nm)
BFae2	5.1	30	X:5.3 Y:5.0 Z:5.1
LcFae8	6.0	30	X:4.3 Y:5.7 Z:4.2
BFae9	5.5	30	X:4.1 Y:4.8 Z:5.2
RaFae	5.9	29	X:4.3 Y:4.7 Z:4.1
CrFae	6.2	33	X:5.6 Y:4.6 Z:4.3
CcFae	5.1	35	X:5.2 Y:4.5 Z:4.4

^a Calculated by ExPASy.

^b Calculated by ExPASy.

^c Determined by homology modelling using Phyre2 (Kelley et al., 2015).

than the protein's pI , the protein surface may still retain enough positively charged patches, which aided the absorption of protein onto the negatively charged surface.

3.2. Screening of synthetic activity of the immobilized FAEs

The immobilized FAEs were assayed for their synthetic activity at pH values ranging from 5 to 9, and the performance was compared to that of the free enzymes. The synthetic activity was assayed in the presence of 1-butanol as an acceptor and methyl ferulate (MFA) as a donor. Because of the enzymatic activity, MFA could be either converted to butyl ferulate (BFA) by transesterification or hydrolyzed to ferulic acid (FA). Since 1-butanol is present in excess, the ferulic acid can, to some extent, be esterified to butyl ferulate. Immobilized FAEs exhibited optimal synthetic activity at pH 7 (Fig. 2A). Of the six candidates, BFae2, LcFae8, BFae9, RaFae and CrFae showed synthetic activity with BFae2, LcFae8, BFae9 and CrFae the four best FAEs showing specific BFA activity ranging from 5 to 14 $\mu\text{M BFA} \cdot \text{min}^{-1} \cdot \text{mg}_{\text{protein}}^{-1} \cdot \text{mg}_{\text{MPS}}^{-1}$. Compared to their non-immobilized counterparts, the specific BFA activity of the immobilized FAEs dropped by nearly one order of magnitude. The specific BFA activity of the free BFae2, LcFae8, BFae9 and CrFae was 60 to 120 $\mu\text{M BFA} \cdot \text{min}^{-1} \cdot \text{mg}_{\text{protein}}^{-1}$ at pH 7 (Fig. 2B). Free RaFae and CcFae were most active at pH 9 and 8, respectively, but the immobilization on SBA-15 had nearly diminished their synthetic activity (Fig. 2B).

3.3. Effect of protein loading on the synthetic activity of the bacterial FAEs

The deterioration of BFA activity following immobilization on SBA-15 suggests the synthetic ability of the bacterial FAEs is susceptible to immobilization. Hence, we implemented three different strategies to possibly increase the synthetic activity by modulating the protein loading and physicochemical properties, i.e. pore sizes and morphologies; and hydrophobic-modified surfaces of the SBA-15. Firstly, we investigated the effect of molecular crowding by increasing protein loading on SBA-15. It has been shown that the performance of an immobilized enzyme could be fine-tuned by increasing the protein loading in MPS (Lei et al., 2008). The four best FAEs BFae2, LcFae8, BFae9 and CrFae that have shown synthetic activity following immobilization on SBA-15 were chosen for further studies (Fig. 2A).

To investigate the protein loading effect, the enzyme dosage for immobilization was gradually increased from 0.4, 0.6, 0.8 to 1.0 g/L in citrate-phosphate buffer, pH 7. The data revealed that BFae2 loading in SBA-15 correlated positively with increasing protein concentration, while CrFae only showed increasing loading from 0.4 to 0.6 g/L, and after that, higher protein concentration during immobilization did not lead to a further increase of protein loading in the support material (Fig. 2C). The loading for BFae9 and LcFae8 was the lowest since the same protein loading was observed regardless of the increasing enzyme concentration used during immobilization. At a 0.4 g/L protein concentration, BFae2 produced only 23% mol BFA and 44% mol FA. When the protein loading increased by 2-fold, the % mol BFA was

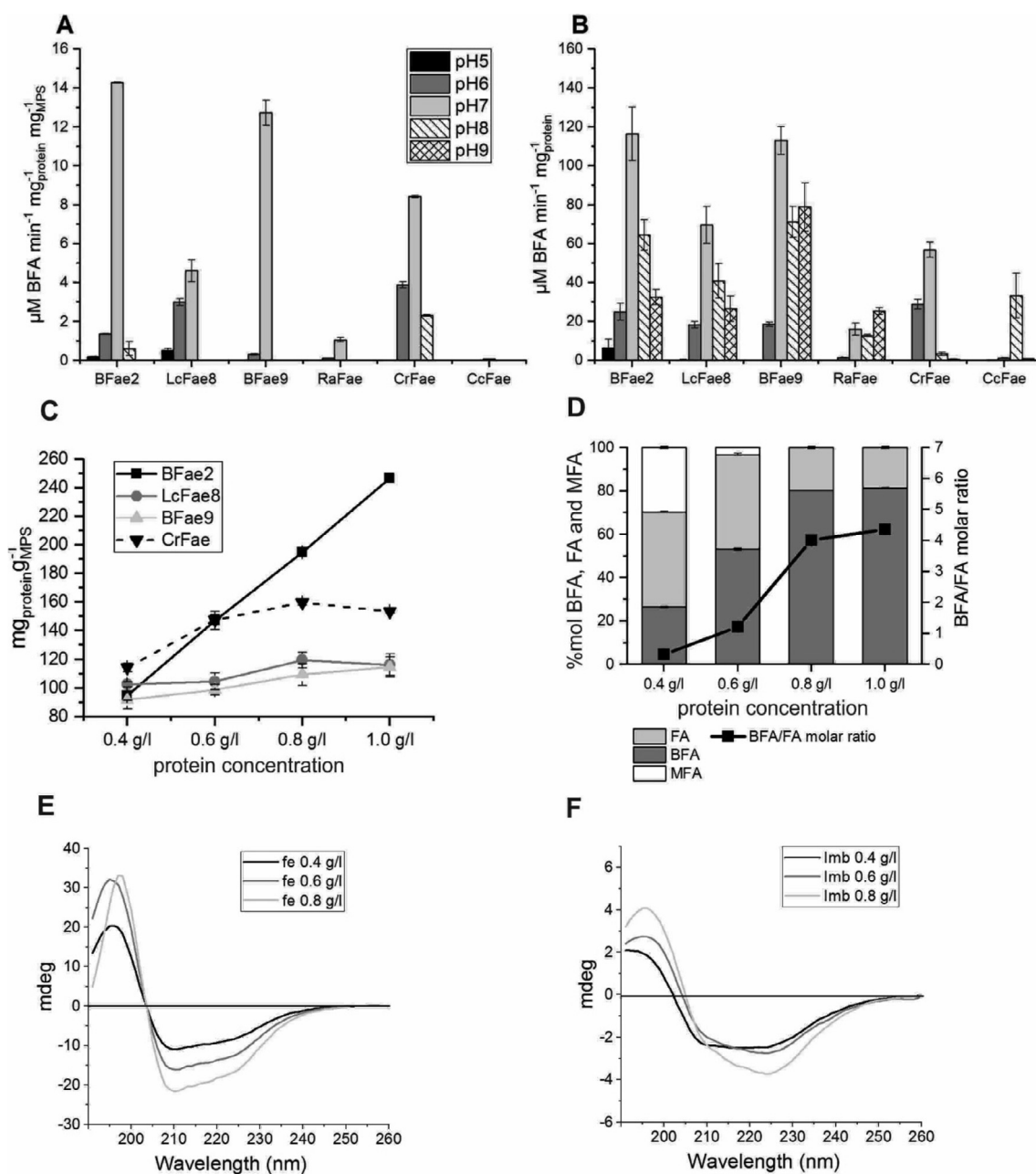


Fig. 2. Comparison of specific BFA activity for (A) immobilized FAEs and (B) free FAEs in solution after 24 h of incubation in 1-butanol/buffer (92.5:7.5, v/v) and 30 mM MFA across a pH range from 5 to 9. (C) Protein loading for BFae2, LcFae8, BFae9 and CrFae when the protein concentration for immobilization increased from 0.4, 0.6, 0.8 to 1.0 g/L. (D) BFae2 showed improved BFA yield when the protein loading increased (SBA-15 with a 10 nm pore size). The formation of BFA and FA; and depletion of MFA were measured after 48 h of incubation at pH7 and 30 °C. The % mol BFA, FA and MFA were calculated by comparing the molar amount of BFA, FA and MFA to total molar amount of BFA + FA + MFA and expressed as percentage. Error bar represents standard deviation of duplicates. (E) Far-UV CD spectra of BFae2 when present as free enzyme in solution and (F) immobilized enzyme in SBA-15 with a 10 nm pore size at protein concentration of 0.4, 0.6 and 0.8 g/L. fe, free enzyme in solution; imb, immobilized enzyme.

dramatically elevated by 3-fold up to 80%, which corresponded to a 13-fold increment of the BFA/FA ratio (Fig. 2D). The protein loading for LcFae8, BFae9 and CrFae was only mildly affected, and thus no change in the % mol BFA was identified. The formation of BFA and FA was followed in a time course assay, revealing that the BFA and FA productivities were accelerated when BFae2 was immobilized at a 0.8 g/L protein concentration. Interestingly, the immobilized enzyme could effectively esterify FA to BFA when the MFA substrate was nearly consumed. The results indicate that the promotion of transesterification and esterification activities contribute to improved % mol BFA at high BFae2 protein loading.

To more deeply understand the effect of protein loading on the

BFae2 secondary structure, we performed circular dichroism (CD) spectroscopic study. The data revealed that the far UV spectra for free BFae2 were unchanged regardless of the increasing protein concentration (Fig. 2E). All three spectra acquired from 0.4, 0.6 and 0.8 g/L protein concentrations exhibited two negative maxima at 208 nm and 222 nm corresponding to α -helical proteins (Greenfield, 2007). In contrast, the far-UV spectrum for the 0.4 g/L protein concentration differed from those acquired from 0.6 and 0.8 g/L for the immobilized BFae2 (Fig. 2F), suggesting that the protein conformation of BFae2 at low protein loading was different from that displayed at high protein loading. Though the spectra for the immobilized BFae2 differ from those acquired from the free enzyme, it is difficult to deduce that the

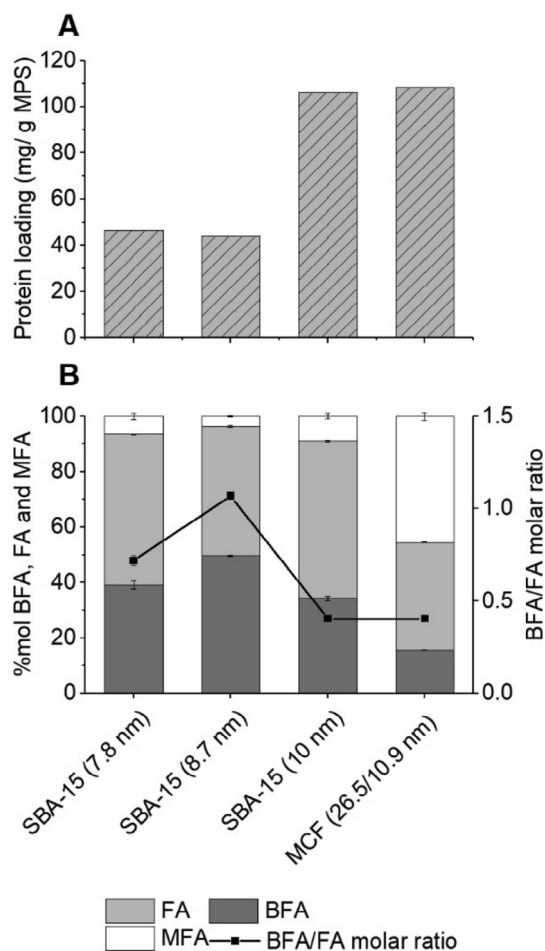


Fig. 3. Effect of pore size on (A) protein loading and (B) % mol BFA, FA and MFA of immobilized BFae2 after 48 h of incubation at pH7 and 30 °C. The % mol of BFA, FA and MFA were calculated by comparing the molar amount of BFA, FA and MFA to total molar amount of BFA + FA + MFA and expressed as percentage. Error bar represents standard deviation of duplicates.

immobilization induces structural changes in BFae2. As the signal intensity for the immobilized enzyme was 5-fold lower, which was probably caused by signal diffraction by particle suspension in solution, the distorted spectrum from the immobilized BFae2 could result from an instrumental measurement artefact. Nonetheless, by comparing the spectra acquired from the immobilized enzyme, which presumably suffer the same level of UV light diffraction due to particle suspension, a clear difference could be seen between low and high protein loading, indicating that the high protein loading on SBA-15 had induced structural changes in BFae2.

3.4. Effect of SBA-15 pore sizes and morphologies on the synthetic activity of BFae2

Since BFae2 demonstrated higher synthetic capacity when it was entrapped in a crowded environment, we further investigated the effect of immobilizing BFae2 on SBA-15 with a pore size smaller than 10 nm, and also using MPS with different pore morphology. It has previously been demonstrated that the relative pore size of MPS to protein dimension influences the catalytic activity of an enzyme. For example, both studies from Sang and Coppens (2011) and Takahashi et al. (2000) demonstrated that more effective enzyme performance could be obtained by using MPS with a pore size closest to the enzyme's molecular dimension.

The estimated size of BFae2 is $5.3 \times 5.0 \times 5.1 \text{ nm}^3$ (Table 2), and

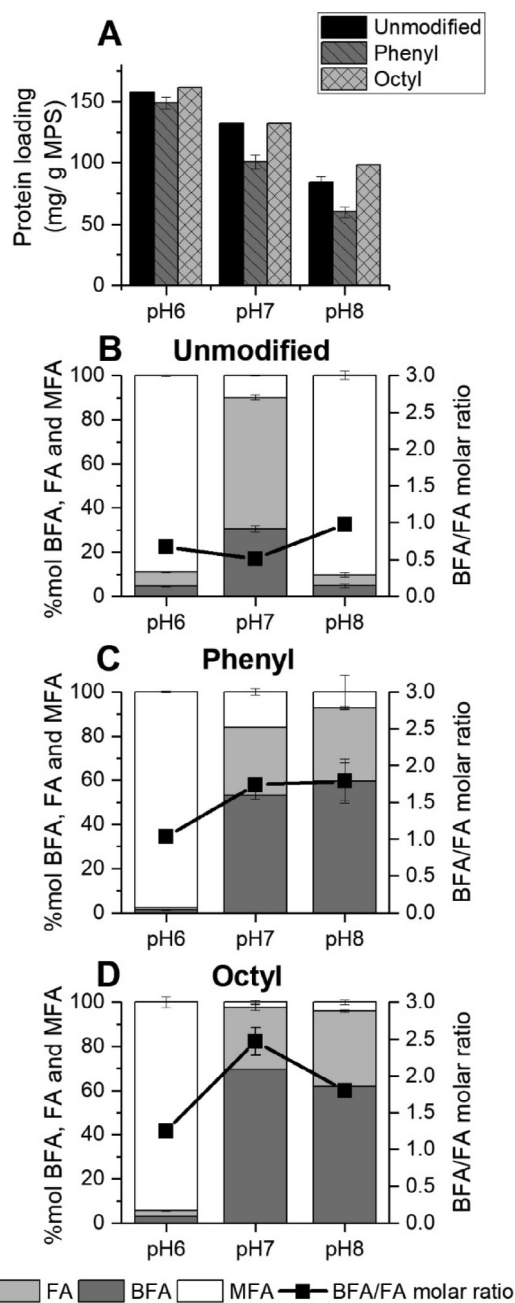


Fig. 4. Effect of hydrophobic-modified surface on (A) BFae2 protein loading across a pH range from 6 to 8. (B) The % mol BFA, FA and MFA obtained from immobilization of BFae2 on unmodified (C) phenyl- and (D) octyl-modified surface after 48 h of incubation at 30 °C. The % mol BFA, FA and MFA were calculated by comparing the molar amount of BFA, FA and MFA to total molar amount of BFA + FA + MFA and expressed as percentage. Error bar represents standard deviation of duplicates.

thus SBA-15 with pore sizes of 7.8 nm, 8.7 nm and 10 nm, as well as MPS with different pore morphology, MCF (26.5 nm/10.9 nm) will have enough window size to allow protein entrance (Table 1). Since the BFae2 immobilized at 0.4 g/l protein concentration produced lowest % mol BFA, this protein loading condition was selected for studying the effect of using pore sizes smaller than 10 nm to circumvent the additive effect contributed from a high protein loading. The BFae2 was efficiently immobilized in 10 nm pore size SBA-15 and MCF, in which, the protein loading was ranging from 106 to 108 $\text{mg}_{\text{protein}} \text{g}_{\text{MPS}}^{-1}$ (Fig. 3A). In contrast, for the SBA-15 with pore sizes of 8.7 nm and 7.8 nm, the protein loading attained was only 44 to 47 $\text{mg}_{\text{protein}} \text{g}_{\text{MPS}}^{-1}$, respectively,

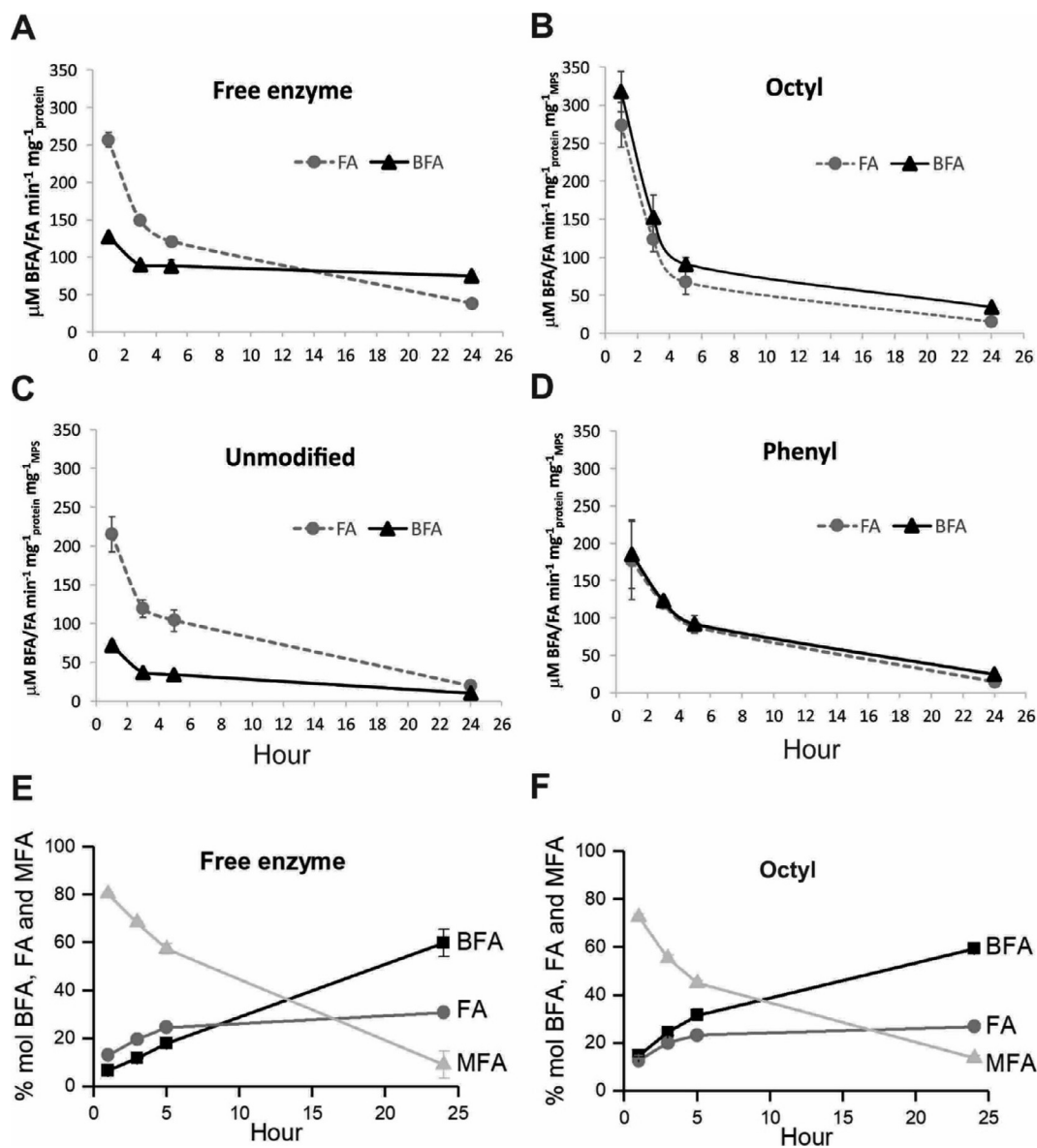


Fig. 5. Specific BFA and FA activity for (A) free BFAe2 in solution and the corresponding enzyme immobilized on SBA-15 with (B) octyl-, (C) unmodified- and (D) phenyl-modified surfaces. (E) Formation of BFA and FA; and depletion of MFA in the presence of BFAe2 as free and (F) immobilized enzyme (octyl-modified SBA-15). The enzyme mixture was incubated for 24 h in the presence of 1-butanol/buffer (92.5:7.5, v/v) and 30 mM MFA at pH 7. Error bar represents standard deviation of duplicates.

indicating that the SBA-15 with pore sizes smaller than 10 nm limited the entrance of BFAe2. Interestingly, despite a lower protein loading, the % mol BFA and the BFA/FA molar ratio obtained from SBA-15 with a 8.7 nm pore size were enhanced compared to those loaded in SBA-15 with a 10 nm pore size, as well as the MCF that possessed a foam-like pore morphology (Fig. 3B). The highest % mol BFA was achieved with BFAe2 loaded in 8.7 nm pore size SBA-15 with a % mol BFA and a BFA/FA molar ratio of 50% and 1.1, respectively. Compared to the performance of the immobilized enzyme on the SBA-15 with a 10 nm pore size, the % mol BFA and the BFA/FA molar ratio increased by 1.1-fold and 2.8-fold, respectively.

Increasing the % mol BFA with SBA-15 of 8.7 nm pore size further proved that the enzyme could perform more effectively when it was encapsulated in a pore size closer to its molecular dimension. The reason could probably be attributed to the pore geometry. Since the degree of curvature of 8.7 nm pore sized SBA-15 is higher than the MPS with a 10 nm pore size, it could create a more pronounced molecular crowding effect presumably leading to conformational changes that

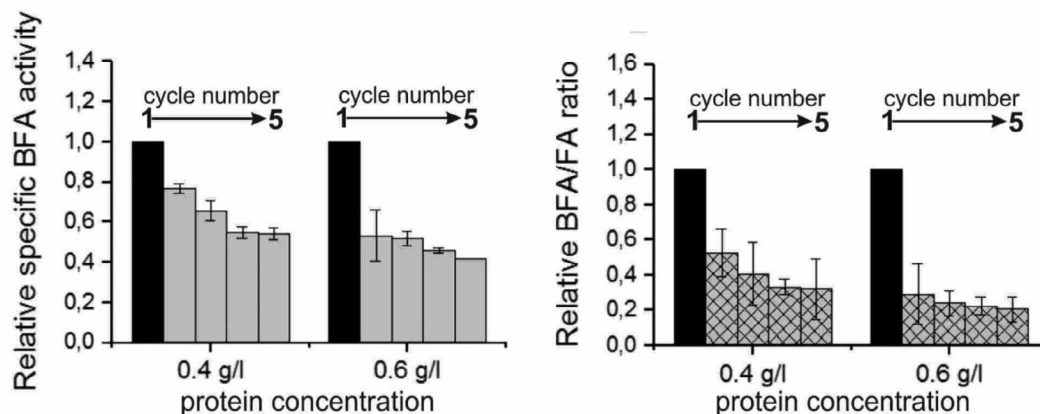
favor synthetic activity. The less compelling result from the 7.8 nm pore sized SBA-15 was probably due to the pore entrance being too small to allow enough protein to enter the pores.

3.5. Effect of hydrophobic surfaces on the synthetic activity of BFAe2

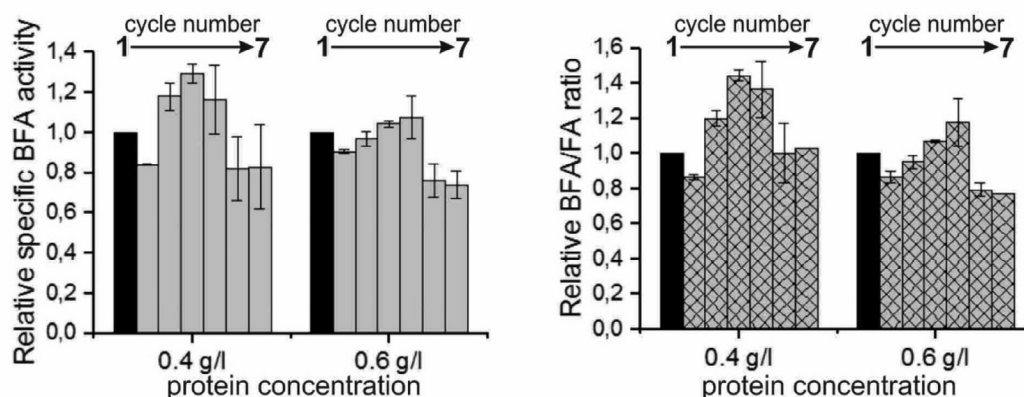
Silica surface modification can also be used to modulate enzymatic activity (Sang and Coppens, 2011; Gomes and Palmqvist, 2017). The silanols on the unmodified surface could be tailored according to the physicochemical properties of the enzyme (Lei et al., 2008) or the reaction conditions. In this study, since the reaction was carried out in the presence of fatty alcohol, we functionalized the surface of SBA-15 with phenyl or octyl moieties to lower the water activity within the pore environment of SBA-15. The hypothesis is that such an environment could mediate the diffusion of 1-butanol more effectively than the unmodified counterpart.

BFAe2 was immobilized at a protein concentration of 0.4 g/L and assayed for the formation of BFA and FA across a pH range from 6 to 8.

A) Unmodified SBA-15 (1.5 ml tube)



B) Unmodified SBA-15 (2 ml tube)



C) Hydrophobic-modified SBA-15 (2 ml tube)

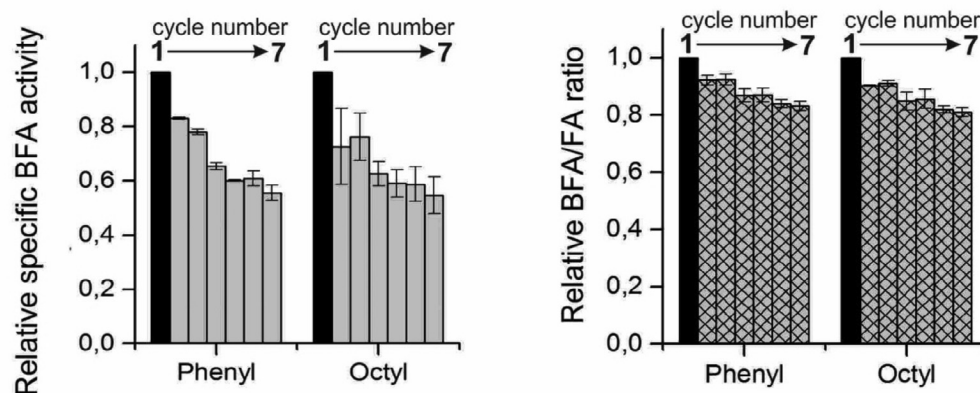


Fig. 6. Reusability of BFAe2 immobilized on SBA-15 with unmodified, phenyl- and octyl-modified surfaces at pH7. For the immobilization of BFAe2 on unmodified SBA-15, the reusability was evaluated by using (A) 1.5 mL and (B) 2 mL Eppendorf tube to compare for the effect of mixing. (C) The synthetic reaction of BFAe2 immobilized on phenyl- and octyl-modified surfaces was carried out in a 2 mL tube. The enzyme recovery was evaluated by comparing the specific BFA activity and BFA/FA ratio in relative to the first reaction cycle. Each reaction cycle lasted 24 h.

The protein loading of BFAe2 on the octyl-modified surface was somewhat comparable to that was immobilized on the unmodified surface (Fig. 4A). The immobilization of BFAe2 on phenyl modified surface was low, especially at pH 7 and 8. Interestingly, both phenyl- and octyl-modified SBA-15 improved the % mol BFA at pH 7 and 8. At pH7, the octyl-modified surface outperformed others since the % mol BFA, and BFA/FA molar ratio was elevated by 2.3- and 5-fold, respectively, compared to the unmodified surface (Fig. 4B–D). Whereas, the phenyl modified surface performed better at pH 8, as the % mol BFA and BFA/FA molar ratio were improved by 12- and 2-fold, respectively, compared to the unmodified counterpart. The result suggests that the

optimal pH for the synthetic reaction was shifted to pH 8 by immobilizing BFAe2 on a phenyl-modified surface. The % mol BFA obtained after 48 h of reaction from the BFAe2 immobilized on octyl- and phenyl-modified SBA-15 was $\approx 70\%$ and 60% , respectively.

In comparison to the free enzyme in solution, the BFA activity at 1st hour of reaction exhibited by the phenyl- and octyl-modified surfaces had been improved by 1.5- and 2.5-fold, respectively (Fig. 5A–D). Thereafter, the enzyme activity reached a plateau after 3 h of reaction. Notably, the modification of SBA-15 with hydrophobic moieties altered the enzyme behavior leading to similar level of BFA and FA activity (Fig. 5B and D). For free BFAe2 (Fig. 5A) or those loaded on unmodified

SBA-15 (Fig. 5C), the enzymatic activity shifted towards hydrolysis at the initial phase of reaction. When the reaction was extended to 24 h, free BFae2 exhibited higher BFA activity than FA activity. The BFA and FA produced via all three surface chemistries were followed in a time course assay. Likewise, the BFA productivity was seemingly driven higher than the FA productivity following immobilization on the octyl surface (Fig. 5F), indicating the promotion of enzyme specificity towards synthetic activity, which was less favorable by the enzyme when it was immobilized on the unmodified surface or present in free form (Fig. 5E). The improved BFA activity at the initial phase of the reaction of octyl-modified surface immobilized enzyme led to comparable % mol BFA obtained with the free enzyme (Fig. 5E–F). We previously determined that BFae2 performed better when it was immobilized in SBA-15 with a pore size closer to its protein dimensions. The pore sizes measured in the octyl- and phenyl-modified SBA-15 were 8.7 nm and 8.2 nm, respectively (Table 1). Thus, the improvement of BFA activity and yield may be contributed by the combined effect of pore size reduction and hydrophobic modification in SBA-15.

This is the first report demonstrating that the synthetic activity of bacterial feruloyl esterase could be enhanced via immobilization on octyl- and phenyl-modified SBA-15 compared to non-modified SBA-15. The support material grafted with hydrophobic moieties has been widely used for the immobilization of lipase to activate its transesterification/esterification activity as the enzyme favorably work in a lipid/water interfacial system due to inherent protein structure (Brzozowski et al., 1991). Therefore, it is worth pursuing further to decipher the protein structure of BFae2, and to analyze the enzyme behavior in a lipid/water interfacial system.

3.6. Reusability of the immobilized BFae2

The immobilized BFae2 was accessed for its stability over repeated reaction cycles at pH 7. The enzyme was first immobilized on the unmodified surface, and the reaction was carried out in 1.5 mL and 2 mL Eppendorf tubes to compare the mixing effect. Two protein concentrations, 0.4 and 0.6 g/L, were used for the immobilization since BFae2 exhibited enhanced synthetic activity at higher protein loading. Thus, we wanted to ascertain if the protein stability was affected by the amount of protein immobilized on SBA-15.

The results clearly showed that the performance of immobilized BFae2 somewhat depended on the tube geometry employed for incubation (Fig. 6A–B). For BFae2 incubated in a 1.5 mL tube, regardless of the amount of protein immobilized on SBA-15, both the BFA activity and the BFA/FA ratio dropped rapidly after one repeated cycle. The BFA activity and the BFA/FA ratio remaining after four repeated cycles were 50% and 30%, respectively, compared to the first reaction cycles. In contrast, the enzyme-support particles were more stable when it was incubated in a 2 mL tube. The BFA activity and BFA/FA ratio retained were consistently higher than 80% in six repeated cycles, regardless of the amount of protein loaded in SBA-15. Interestingly, for the BFae2 immobilized at a 0.4 g/L protein concentration, the BFA activity and the BFA/FA ratio dropped approximately 10–20% after one repeated cycle. Following this, it increased 20–40% over three repeated cycles. It was unclear why enhanced BFA activity was observed under such conditions. The geometry of the tube bottom probably attributes to the increment, since more space is available in the 2 mL tube bottom. Thus, the enzyme-silica particles probably disperse more effectively in the alcoholic buffer. The results indicate that the homogenous mixing of the enzyme-silica particles is an important factor that determines the reusability of the immobilized enzyme.

The BFae2 immobilized on the hydrophobic surface was tested for its reusability (Fig. 6C). The BFA activity remained 80% after two repeated cycles, and it stayed above 60% over the remaining four repeated cycles. On the other hand, the BFA/FA ratio consistently remained above 80% compared to the level of the first cycle. The performance of both phenyl- and octyl-modified surfaces were similar.

4. Conclusion

Of the six bacterial FAEs tested for their synthetic ability following immobilization on SBA-15, BFae2 showed the highest BFA activity. The immobilized BFae2 favored a crowded environment within the pore of SBA-15 for high synthetic activity. Furthermore, the immobilization of BFae2 on the SBA-15 with phenyl- and octyl-modified surfaces led to a marked improvement of BFA activity and yield. Taken together, the modulation of SBA-15 pore size and hydrophobic-surface is essential to optimize the synthetic activity of the BFae2. The immobilized BFae2 retained a high synthetic activity despite undergoing multiple reaction cycles, demonstrating the robustness of the immobilized enzyme.

Acknowledgements

The authors gratefully acknowledge Dr. Sandra Rocha for providing technical assistant in CD measurement, Professor Pernilla Wittung Stafshede and Professor Bengt Nordén for discussion about the CD results and Professor Anders Palmqvist for providing the MPS material. This work was supported by a grant from the EU FP7 framework [613868, OPTIBIOCAT]

Appendix A. Supplementary data

Supplementary data to this article can be found online at <https://doi.org/10.1016/j.biortech.2019.122009>.

References

- Barrett, E.P., Joyner, L.G., Halenda, P.P., 1951. The determination of pore volume and area distributions in porous substances. I. Computations from nitrogen isotherms. *J. Am. Chem. Soc.* 73, 373–380.
- Bradford, M.M., 1976. A rapid and sensitive method for the quantitation of microgram quantities of protein utilizing the principle of protein-dye binding. *Anal. Biochem.* 72, 248–254.
- Brunauer, S., Emmett, P.H., Teller, E., 1938. Adsorption of gases in multimolecular layers. *J. Am. Chem. Soc.* 60, 309–319.
- Brzozowski, A.M., Derewenda, U., Derewenda, Z.S., Dodson, G.G., Lawson, D.M., Turkenburg, J.P., Bjorkling, F., Huge-Jensen, B., Patkar, S.A., Thim, L., 1991. A model for interfacial activation in lipases from the structure of a fungal lipase-inhibitor complex. *Nature* 351, 491–494.
- Essa, H., Magner, E., Cooney, J., Hodnett, B.K., 2007. Influence of pH and ionic strength on the adsorption, leaching and activity of myoglobin immobilized onto ordered mesoporous silicates. *J. Mol. Catal. B Enzym.* 49, 61–68.
- Fernandez-Lafuente, R., Armisen, P., Sabuquillo, P., Fernández-Lorente, G., Guisán, M.J., 1998. Immobilization of lipases by selective adsorption on hydrophobic supports. *Chem. Phys. Lipids* 93, 185–197.
- Gomes, M.Z.d.V., Palmqvist, A.E.C., 2017. Influence of operating conditions and immobilization on activity of alcohol dehydrogenase for the conversion of formaldehyde to methanol. *New J. Chem.* 41, 11391–11397.
- Greenfield, N.J., 2007. Using circular dichroism spectra to estimate protein secondary structure. *Nat. Protocols* 1, 2876–2890.
- Gustafsson, H., Thörn, C., Holmberg, K., 2011. A comparison of lipase and trypsin encapsulated in mesoporous materials with varying pore sizes and pH conditions. *Colloids Surf. B Biointerfaces* 87, 464–471.
- Hartmann, M., Kostrov, X., 2013. Immobilization of enzymes on porous silicas – benefits and challenges. *Chem. Soc. Rev.* 42, 6277–6289.
- Hüttner, S., Gomes, M., Z.S.V., Iancu, L., Palmqvist, A., Olsson, L., 2017. Immobilisation on mesoporous silica and solvent rinsing improve the transesterification abilities of feruloyl esterases from *Myceliophthora thermophila*. *Bioresour. Technol.* 239, 57–65.
- Kelley, L.A., Mezulis, S., Yates, C.M., Wass, M.N., Sternberg, M.J.E., 2015. The PyMol web portal for protein modeling, prediction and analysis. *Nat. Protocols* 10, 845–858.
- Klibanov, A.M., 2001. Improving enzymes by using them in organic solvents. *Nature* 409, 241–246.
- Lei, C.H., Thereza, A.S., Shin, Y.S., Liu, J., Ackerman, E.J., 2008. Enzyme specific activity in functionalized nanoporous supports. *Nanotechnology* 19, 125102.
- Lukens, W.W., Schmidt-Winkel, P., Zhao, D., Feng, J., Stucky, G.D., 1999. Evaluating pore sizes in mesoporous materials: a simplified standard adsorption method and a simplified Broekhoff–de Boer method. *Langmuir* 15, 5403–5409.
- MacKenzie, C.R., Bilous, D., Schneider, H., Johnson, K.G., 1987. Induction of cellulolytic and xylanolytic enzyme systems in *Streptomyces* spp. *Appl. Environ. Microbiol.* 53, 2835–2839.
- MacKenzie, C.R., Bilous, D., 1988. Ferulic acid esterase activity from *Schizophyllum commune*. *Appl. Environ. Microbiol.* 54, 1170–1173.
- Moerz, S.T., Huber, P., 2014. Protein adsorption into mesopores: a combination of electrostatic interaction, counterion release, and van der Waals forces. *Langmuir* 30, 2729–2737.

- Oosterveld, A., Beldman, G., Schols, H.A., Voragen, A.G.J., 2000. Characterization of arabinose and ferulic acid rich pectic polysaccharides and hemicelluloses from sugar beet pulp. *Carbohydr. Res.* 328, 185–197.
- Sang, L., Coppens, M., 2011. Effects of surface curvature and surface chemistry on the structure and activity of proteins adsorbed in nanopores. *Phys. Chem. Chem. Phys.* 13, 6689–6698.
- Schmidt-Winkel, P., Lukens, Wayne W., Yang, P., Margolese, D.I., Lettow, J.S., Ying, J.Y., Stucky, G.D., 2000. Microemulsion templating of siliceous mesostructured cellular foams with well-defined ultralarge mesopores. *Chem. Mater.* 12, 686–696.
- Secundo, F., 2013. Conformational changes of enzymes upon immobilisation. *Chem. Soc. Rev.* 42, 6250–6261.
- Sequeira, A.F., Guerreiro, C.I.P.D., Vincentelli, R., Fontes, C.M.G.A., 2016. T7 Endonuclease I mediates error correction in artificial gene synthesis. *Mol. Biotechnol.* 58, 573–584.
- Srinivasan, M., Sudheer, A.R., Menon, V.P., 2007. Recent advances in Indian herbal drug research. ferulic acid: therapeutic potential through its antioxidant property. *J. Clin. Biochem. Nutr.* 40, 92–100.
- Takahashi, H., Li, B., Sasaki, T., Miyazaki, C., Kajino, T., Inagaki, S., 2000. Catalytic activity in organic solvents and stability of immobilized enzymes depend on the pore size and surface characteristics of mesoporous silica. *Chem. Mater.* 12, 3301–3305.
- Thörn, C., Gustafsson, H., Olsson, L., 2011. Immobilization of feruloyl esterases in mesoporous materials leads to improved transesterification yield. *J. Mol. Catal. B Enzym.* 72, 57–64.
- Thörn, C., Udatha, D.B.R.K.G., Zhou, H., Christakopoulos, P., Topakas, E., Olsson, L., 2013. Understanding the pH-dependent immobilization efficacy of feruloyl esterase-C on mesoporous silica and its structure–activity changes. *J. Mol. Catal. B Enzym.* 93, 65–72.
- Topakas, E., Vafiadi, C., Christakopoulos, P., 2007. Microbial production, characterization and applications of feruloyl esterases. *Process Biochem.* 42, 497–509.
- Vinu, A., Streb, C., Murugesan, V., Hartmann, M., 2003. Adsorption of cytochrome C on new mesoporous carbon molecular sieves. *J. Phys. Chem. B* 107, 8297–8299.
- Zaks, A., Klibanov, A.M., 1985. Enzyme-catalyzed processes in organic solvents. *Proc. Natl. Acad. Sci. U.S.A.* 82, 3192–3196.
- Zhou, H., Dill, K.A., 2001. Stabilization of proteins in confined spaces. *Biochem* 40, 11289–11293.
- Zhou, Z., Hartmann, M., 2012. Recent progress in biocatalysis with enzymes immobilized on mesoporous hosts. *Top. Catal.* 55, 1081–1100.